SIMULATION OF FERROCEMENT ELEMENTS UNDER IN-PLANE SHEAR

Apostolos Koukouselis and Euripidis Mistakidis

[1]Laboratory of Structural Analysis and Design, Department of Civil Engineering
University of Thessaly, Volos, GR-54124, Greece
e-mail: akoukouselis@gmail.com ; web page: http://lsad.civ.uth.gr

Keywords: Ferrocement; in-plane shear; Nonlinear modelling; Composite Layered Shells.

Abstract. *Ferrocement is a type of reinforced concrete widely used in the construction of thin shell elements. This study investigates a simulation method based on composite layered shells for the nonlinear analysis of ferrocement elements under in-plane shear. A tube torsion test is simulated and analyzed with MSC MARC and its results are compared to an alternate calculation method, the Simplified Model for Combined Stress resultants (SMCS) as well as with experimental data. The simulation method is found to produce accurate results for fully under-reinforced elements with a range of strong to weak reinforcement ratios less than 2.*

1 INTRODUCTION

Ferrocement, a form of reinforced concrete that uses as reinforcement multiple layers of closely spaced steel meshes of small diameter, is a material widely used in the construction of thin shell structures. In many cases, the ferrocement structural elements mostly act as membrane elements not only under axial loading but also under in-plane shear. Over the years theories and methods were developed for calculating the ultimate shear strength of reinforced concrete (R/C) panels and predicting their behavior under pure shear or combined axial and shear stresses. For many years the design of such elements was governed by the assumption that the inclination of the cracks with respect to the loading vector was equal to 45 degrees. Such an assumption, although correct in cases where the panel is subjected to pure shear and is equally reinforced in both directions, is very conservative and in general underestimates the load carrying capacity of the elements.

The Compression Field Theory (CFT) [1] [2], introduced the idea of the correlation of the inclination angle of the crack with respect to the loading axis to the strain conditions of the element. Then, Vecchio and Collins [3], based on an experimental program also utilized in this study, developed the Modified Compression Field Theory (MCFT) introducing the contribution of concrete by its tensile stress in the ultimate shear resistance of the element. Due to the complexity of its equation, MCFT was found by engineers to be a very cumbersome method to be used in hand calculations, thus, simplified methods were developed. The simplified MCFT (SMCFT) by Bentz et al. [4] simplifies the calculations of MCFT based on various assumptions, one of which is the lack of axial stress in the transverse direction. Thus, SMCFT is limited to the cases of shear under uniaxial loading.

A very effective calculation method was proposed by Rahal [5] termed SMCS (Simplified Model for Combined Stress Resultants). The later method correlates the ultimate shear strength and the mode of failure to the reinforcement indices and ultimate concrete compressive strength. Combined with the calculation method proposed by the same author [6] regarding the determination of the post-cracking shear modulus of the reinforced concrete panel, SMCS can effectively describe the behavior of R/C membrane elements under in plane shear.

Another effective approach for predicting the behavior of shear panels is the application of numerical procedures such as the Finite Element Method. This approach can either be applied in the form of linear analysis, by using effective properties for the membrane elements, or in the form of nonlinear analysis, by incorporating in the models nonlinear material stress-strain relationships. For the nonlinear analysis of R/C elements, simulation methods and guidelines exist for decades. Bergan and Holand [7], for example, mention two simulation techniques, one based on the use of shell elements to simulate the cement mortar matrix (degenerating to plain stress elements in case of 2D problems) and beam elements to simulate the reinforcing rods and mesh and another one based on the use of composite layered shell elements. Between these two methods, the most effective one seems to be the later, as the first one not only introduces mesh limitations, on the grounds that the shell and beam elements need to be combined at common nodal points, but also makes it difficult to simulate the position of the rods along the thickness of the element.

In the present paper, the simulation method based on composite layered shells for the nonlinear analysis of

ferrocement elements under in plane pure shear is investigated. A tube torsion test is simulated and analyzed in MSC Marc [8] and its results are compared to those calculated by the SMCS and experimental data. The findings of this investigation are expected to provide certain guidelines for the simulation of ferrocement membrane elements under shear, help determine possible limitations of this simulation technique and can constitute the basis for future experimental and numerical research on the design and analysis of ferrocement structures. Section 2 provides the basic information needed by the reader regarding the Simplified Model for Combined Stress resultants while Section 3 summarizes the past experimental works on the behaviour of R/C panels under in-plane shear. The results of these tests are used for the verification of the proposed simulation method. Section 4 provides a detailed description regarding the formulation of the numerical simulation models used in the present paper. Finally, Section 5 further investigates the composite layered shell simulation method by comparing its results to experimental ones, while Section 6 summarizes the findings of the paper and presents its conclusions.

2 FUNDAMENTALS OF THE SMCS

As mentioned in the introduction, SMCS [5] is a simplified method for the calculation of the shear capacity as well as for the prediction of the mode of failure of membrane elements under shear and biaxial normal stresses. The method is based on the compatibility of strains, equilibrium of forces and experimental data, while the existence of normal stresses is taken into account by the concept of superposition of reinforcement (one portion resisting normal loads and one resisting shear ones). SMCS neglects the contribution of the reinforcements beyond a "balanced" limit κ derived from experimental results. Based on this limit, three types of elements and modes of failures exist. Fully under-reinforced (UR) elements in which the ultimate shear strength is attained when both the longitudinal and transverse reinforcement yield, partially under-reinforced ones (PUR) in which at failure the reinforcement in only one direction has yielded and fully over-reinforced (OR) in which failure occurs due to crushing of the concrete matrix before yielding of steel in either direction.

According to Rahal, the nominal shear strength of the elements is calculated as follows:

$$\frac{\tau_n}{f_c^{'}} = \sqrt{\omega_x \omega_y} \le \kappa \tag{1}$$

$$\omega_x = \frac{\rho_x f_{y,x} - \sigma_x}{f_c^{'}} \le \kappa \tag{2a}$$

$$\omega_y = \frac{\rho_y f_{y,y} - \sigma_y}{f_c^{'}} \le \kappa \tag{2b}$$

$$\kappa = \frac{1}{3} - \frac{f_c^{'}}{900} \tag{3}$$

Equations (1) to (3) demonstrate the simplicity of the method. The ultimate shear strength τ_n of a membrane element can be easily calculated by specifying the compressive strength of the concrete $f_c^{'}$, and calculating the reinforcement indices ω_x and ω_y by specifying the reinforcement ratio ρ_i, the reinforcement yield stress $f_{y,i}$ and the normal stress σ_i in each direction. For the classification of the element and the prediction of the failure mode only the two checks of Eq. (2a) and (2b) are needed. The comparison of the SMCS to experimental results (available in [5]) demonstrated the very good performance of the method, which is similar to the other widely used ones (MCFT and SMCFT). In order to better describe the behavior of membrane elements under shear, Rahal [6] correlated the in plane shear modulus of the cracked section G_{cr} to the same parameters, by the use of equation:

$$\frac{G_{cr}}{f_c^{'}} = 135.4\sqrt{\omega_x \omega_y}\ . \tag{4}$$

The reinforcing indices are again limited by κ. Equation (4) applies to all three types of elements (UR, PUR, OR) but is limited to the cases of pure shear ($\sigma_x = \sigma_y = 0$) and evenly distributed reinforcement. The proposed equation was compared by Rahal [6] to available experimental results for pure shear and was found to capture the overall behavior of the membrane elements very well. In Eq. (4) G_{cr} is the best straight line fit produced by regression analysis of the experimental data points between cracking and first yielding. Points between the cracking shear stress τ_{cr} and $1.2\,\tau_{cr}$ are considered to be in the transition zone and are excluded. Although SMCS was developed for conventional reinforced concrete elements, due to the lack of a more ferrocement-specific method, it is used here as a reference solution for the comparison of the results obtained by

the numerical analyses demonstrated later in this study.

3 SYNOPSIS OF PAST EXPERIMENTAL WORK USED IN THIS PAPER

For the validation of the methods and theories referenced in the introductory part of the paper, a variety of experimental data has been used. As nowadays high performance cementitious materials are used in ferrocement structures, this study focuses on cases where the concrete matrix is of high compressive strength (higher than 40MPa). Moreover, this study is limited to fully under-reinforced elements under pure shear. Again, although the experiments were conducted on conventionally reinforced elements, due to lack of more relevant experimental results, they are used as reference for the needs of this investigation. Table 1 summarizes the experimental results used in this study.

Pang and Hsu [9] tested thirteen square 1.4x0.178 m concrete panels in a $\pm 45^0$ tension-compression test. Series A specimens were equally reinforced in both directions while those of series B were unequally reinforced. In both groups the loading in the two directions (tension and compression) was equal. As the authors mention, the scope of series A tests was to study the effect of the reinforcement ratio while that of series B was to investigate the effect of the ratio of transverse to longitudinal reinforcement. From their experimental program, specimens A2, A3 and B1 to B3 are used for comparison reasons in Section 5.

Vecchio et al. [10] in the University of Toronto tested 12 panels in pure shear and shear with biaxial stresses. The specimens were 0.89x0.89x0.07 m and the loading was monotonic and proportional. Two series of experiments were carried out named *"PHS"* and *"PA"* with the *"PHS"* being more heavily reinforced. From the six specimens tested in pure shear, only PA1 and PA2 are used here as, according to Eq. (2a), the other four are partially under-reinforced and thus have a failure mode outside the limitations of this investigation.

The HB, VA and VB series 1.4x1.4x0.178 m panels tested in the University of Houston were used to validate and generalize the constitutive laws for the softened truss models proposed by Hsu and Zhang [11], [12]. As with the previous experimental programs, cases of fully under reinforced specimens were chosen for the comparison with the composite layered shell simulation method. Specimens VA1, VA2 and VA3 present equal reinforcing indices in both directions, while HB3, HB4, VB1, VB2 and VB4 are more heavily reinforced along the *x* direction.

Experiment	Specimen	$f_c^{'}$	ω_x	ω_y	κ
Pang and Hsu (1995) 1.4x1.4x0.178m	A2	41.3	0.134	0.134	0.287
	A3	41.7	0.192	0.192	0.287
	B1	45.3	0.123	0.059	0.283
	B2	44.1	0.181	0.126	0.284
	B3	44.9	0.178	0.059	0.283
Vecchio et al. (1994) 0.89x0.89x0.07m	PA1	49.9	0.173	0.086	0.278
	PA2	43	0.202	0.100	0.286
Hsu and Zhang (1997) 1.4x1.4x0.178m	HB3	66.8	0.120	0.040	0.259
	HB4	62.9	0.223	0.042	0.263
Hsu and Zhang (1998) 1.4x1.4x0.178m	VA1	95.1	0.056	0.056	0.228
	VA2	98.2	0.100	0.100	0.224
	VA3	94.6	0.173	0.173	0.228
	VB1	98.2	0.100	0.054	0.224
	VB2	97.6	0.167	0.055	0.225
	VB4	96.9	0.085	0.028	0.226

Table 1. Summary of the experiments

4 NUMERICAL SIMULATION BY THE USE OF COMPOSITE LAYERED SHELLS

Although hand calculations are always useful for preliminary design as well as for validation, nowadays most of the analysis and design process is computer assisted, as engineers are called to analyze and design more and more complex structures. As far as ferrocement structures are concerned, which are usually free form shell structures, they are in most cases modeled by the use of shell elements rather than solid ones so that the computational cost is reduced. Thus, two methods seem appropriate for the simulation of the composite material.

The first one uses shell elements to simulate the concrete matrix and beam elements for the reinforcing rods (mixed elements model). In the second one composite layered shells are used for the simulation of the entire cross section. As mentioned in the Introduction, the first method introduces mesh limitations as the shell and beam elements need to have common nodes. Moreover, the position of the reinforcement along the thickness of the element is more difficult to be simulated, as beam offsets have to be used. Thus, the simulation by the use of composite layered shell has an obvious advantage as far as the simulation of the bending behavior is concerned. This study investigates the later simulation technique in the case of pure shear and compares its results to analytical and experimental ones.

A tube torsion test is simulated in MSC Marc [8]. As Chaterjee S. et al. [13] mention, torsion tests on thin tubes have been suggested by many investigators as an effective method for determining the in plane shear behavior of composite materials. Thus, thin ferrocement tubes are modeled and analyzed with height to diameter ratio 2.62 (greater than 2 is generally recommended). The thickness to diameter ratio t/d is 0.018 in all cases investigated, (smaller than 0.02) so that the variation of the shear stress through the thickness is small enough, as suggested by the report of Chaterjee S. et al. [13], while the perimeter to thickness ratio is 174. The models consist only of thin shell elements (MARC element type 139) with a mesh division of 60x50 elements (along the circumference and height respectively). The models are solved using a Full Newton-Raphson iterative procedure, small strain theory and the convergence testing is based on the residual forces. Because at the outer edges of the specimens stress concentrations and numerical convergence issues might arise, the last series of finite elements is considered to be elastic. Even in real experiments, the regions near the grips of the testing machine are usually thicker so that the load is introduced evenly and premature failure is avoided. Only the circumferential displacements are restrained while the radial displacements as well as the rotations of the edges are considered free so that no stresses, other than that of pure shear, appear.

As aforementioned, the composite layered shell model simulates the reinforced section by the use of appropriately arranged layers. Isotropic cement layers are used for the matrix while the reinforcing rods are simulated by equivalent layers of steel. The material of the steel layers, although based on the properties of the reinforcing steel, has to be orthotropic in order for the layers to have stiffness only in the direction of the reinforcing rods. The Poisson's ratio n_{12} is also considered to be equal to zero as deformation in one direction does not cause deformation in the other one. Depending on whether the steel layer represents reinforcement parallel to the local x or the local y axis, it is orientated with an angle of 0 or 90 degrees with respect to the vertical axis respectively. Figure 1 shows a typical composite layered shell used in the analyses.

The constitutive law for both materials was considered bilinear elastic perfectly plastic. The reinforcement steel is assumed to yield at a stress of 500 MPa and has an elasticity modulus along the main direction of 200GPa. For concrete, a modified version of the Buyukozturk criterion is used, which takes into account the onset of cracking. More specifically, the yield surface is based on equation (4) in Buyukozturk [14], while a tension cut-off criterion is also introduced leading to the surface shown in Figure 2.

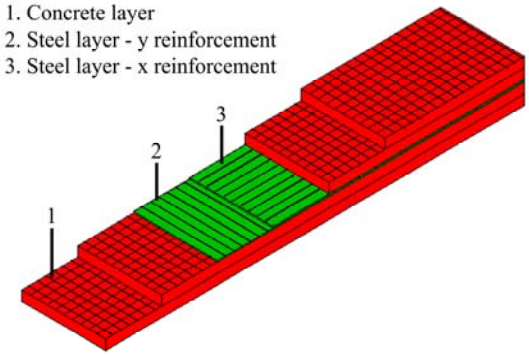

Figure 1. Typical Composite layered shell element.

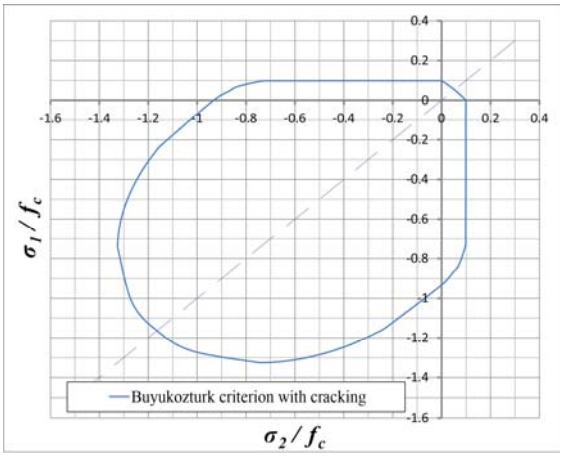

Figure 2. Buyukozturk criterion with cracking [14]

The compressive strength $f_c^{'}$ was equal to 60 MPa while the tensile strength was equal to 3.1 MPa. The elastic modulus was assumed to be equal to 39 GPa and the Poisson's ratio equal to 0.2 Cracking is handled through the smeared crack approach. This approach is very convenient as no remeshing is required and in the case of cracks of small width and smeared throughout the element, such as ferrocement ones, it is known to work well. The orientation of the crack is not needed to be known "*a priori*" as the model orientates the crack to

be parallel to the principal tensile strain while upon cracking the isotropic behavior is converted to orthotropic. The stiffness with respect to the principal tensile stress is reduced by a factor which is a function of the cracking strain (ε_{cr}). The inclination angle θ of the cracks is fixed upon cracking and is not recalculated in each increment, while a second crack can only be formed perpendicularly to the first one.

To fully describe the post cracked behavior of concrete, the post cracking shear modulus needs to be determined. A common assumption is to assume that cracked concrete loses its capability to carry shear stresses upon cracking and thus the shear modulus drops to zero. However, such an assumption is far from reality and involves a sudden transition from a linear isotropic material to an orthotropic one with zero shear stiffness, causing numerical convergence issues and limiting the ability of the model for stress redistribution [15]. In reality, cracked concrete can still transfer shear stresses through aggregate interlock and dowel effect. The post cracked shear modulus of concrete is usually considered to be equal to a percentage of the elastic one $\beta G_{el,c}$, where β is the shear retention factor, ranging from 1 to 0. As Hu and Schnobrich [16] mention, analytical results demonstrated that the value chosen for β is not critical but a value greater than zero is required for numerical instabilities to be avoided. Figure 3 demonstrates a comparison of four analyses with different shear retention factors of the specimen PA1 which has a ratio of reinforcement indices ω_x/ω_y equal to 2.01. It can be observed that the different shear retention factors cause a difference in the behavior of the model after the yielding of the horizontal reinforcement but the ultimate shear strength is the same for all the considered shear retention values. When the reinforcement indices are equal, the effect of the shear retention factor is insignificant, as both directions yield simultaneously. Note that the use of the shear retention factor may cause the tension cut-off criterion to be violated.

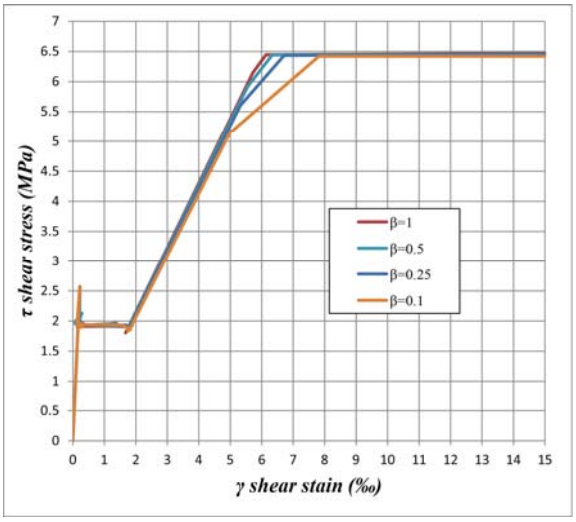

Figure 3. Effect of shear retention factor on the behavior of the model.

5 APPLICATION OF THE COMPOSITE LAYERED SHELL METHOD FOR THE SIMULATION OF EXISTING EXPERIMENTAL RESULTS

This section investigates the performance of the model, by comparing its results for various reinforcement ratios per direction versus experimental ones. Moreover, the numerically obtained results are compared with those calculated by the simplified formulas of SMCS. It should be noted that the actual tested specimens were squares of various dimensions. For the needs of the comparison presented in this section, all experiments were converted to equivalent tube torsion tests (p/t=300, h/d = 2.6). As input for the analyses, only the ultimate compressive concrete strength $f_c^{'}$ and the reinforcement indices ω_x and ω_y were used. The ultimate tensile strength f_{ctm} and concrete yielding strain ε_{c3} were calculated according to Table 3.1 of EN1992 [17] while E_c was based on Figure 3.4 of EN1992 (f_c/ε_{c3}). The softening modulus for cracking was considered to be 10% of E_c . The yield stress of the reinforcing steel was considered to be 500 MPa regardless of the actual used steel for the experiments. Thus, for given reinforcement indices ω_x and ω_y and ultimate compressive strength $f_c^{'}$, the

reinforcement ratios of the equivalent models were determined as $\rho_i = \omega_i f_c / f_y$. The thickness of the steel layer was calculated as $t_i = \rho_i t_{tot}$, where t_{tot} is the total thickness of the composite shell . Regarding shear retention, two values of β were used, namely 0.15 and 0.25, in order to study the effect of this factor on the analysis results.

The above simulation procedure was followed so that all experiments are studied within a unified context and, as in the SMCS, the input is limited to easy to access data to the designer ($f_c^{'}$, ω_x and ω_y). Hence, these analyses are not to be seen only as a virtual reproduction of the experiments but also as a demonstration of a numerical analysis procedure, based on the basic properties of the materials and guidelines widely followed for the design of R/C structures.

Tables 2 and 3 and Figures 4 to 7 present the comparison of the model results to the experimental ones and to the SMCS calculations. Table 2 compares the shear strength calculated by the model to the ones of the corresponding experiment and the prediction of the SMCS. When the reinforcement indices in the two directions are equal, the numerical (model) and analytical (SMCS) results are in very good agreement (Specimens A2, A3 and VA1 to VA3). The agreement of the numerical analyses to the experimental results and analytical solution continues for a ratio of reinforcements ω_x/ω_y up to 2. In these cases, the differences that result are less than 10% (specimens PA1, PA2, B1, B2 and VB1). When the reinforcement ratio is near to 3, the differences of the results range from 8% to 18% while for a ratio of 5 (HB4) the difference between experiment and model reaches 52%. The difference between the analytical solution and the analysis is of the order of 33%.

In more detail, comparing the numerical analyses to the results calculated by SMCS, it is obvious that as the ratio of longitudinal to transverse reinforcement increases, so does the error between the SMCS and the model. The source of this error is the violation of the cracking criterion due to the used shear retention factors. The more the difference between the reinforcement ratios, the more intense crack reorientation is needed in the model for the maximum shear stress to be attained. As crack reorientation is achieved through the development of concrete shear stresses along the crack, that means that in the models of high ω_x/ω_y ratios the concrete shear stresses are higher and so is the violation of the cracking criterion. The produced tensile forces cause the increase of the ultimate shear stress.

As far as the post-cracking shear modulus is concerned, the numerical models are generally stiffer than the analytical solution and the experiments. As in SMCS, the post cracking shear modulus is obtained by a regression analysis as the best straight line fit for the data between $1.2\,\tau_{cr}$ and first yield. The slope of this branch, as observed in Figure 3, is almost independent of the selected shear retention factor and, thus, the post cracking shear modulus G_{cr} of the numerical models is also independent of the used shear retention values. The average difference of the models to the SMCS is 31%. Compared to the experiments, the analyses present a G_{cr} which is about 29% higher (Table 3). A closer look at the overall response of the specimens provided by Figures 4 to 7, leads to the conclusion that apart from the cases where ω_x/ω_y is greater than 2, the response of the numerical models is not much different from the experimental ones. The difference in the post cracking modulus is caused by the fact that defining G_{cr} as the slope of the post-cracking and pre-yielding branch, may be absolutely correct in the cases in which ω_x/ω_y = 1, however, when $\omega_x \neq \omega_y$ there exists an additional branch (between the *y*-reinforcement and *x*-reinforcement yielding) which can be very significant. The numerical models, in contrast to SMCS, reproduce the change of shear stiffness after the yielding of the weak direction and thus, describe in a better way the overall behavior of elements with a reinforcement ratio between 1 and 2.

This branch between yields is highly dependent on the assumptions regarding shear retention (notice that two values regarding β were investigated, 0.15 and 0.25). The different shear retention factor causes no change in the analysis results for the specimens with reinforcement ratio of 1 (A2 to VA3) but affects the behavior of specimens with a ratio between 1 and 2. The cases in which ω_x/ω_y is greater than 2, although presented in the detailed discussion later in this section, are of less importance at this stage of the investigation, on the grounds that their ultimate shear strength is overestimated and thus the range of application of the presented method has to be narrowed to elements with reinforcement ratios up to 2.

Figure 4 compares the stress-strain curves obtained for the Series A experiments by Pang and Hsu [9] to the numerical ones. The three stages mentioned by the authors (elastic uncracked, post-cracking elastic and plastic stage after yielding) are also visible in the numerically obtained curve. The authors also noted that both longitudinal and transverse reinforcement had yielded and the specimens ultimately failed due to crushing of the concrete (descending branch). Based on this fact, one may come to the conclusion that the analyses fail to predict the correct failure mode. However, Pang and Hsu also noted that after yielding, the increase of shear deformation was rapid. In addition, the value of the yielding and the maximum shear stress are very close and thus the failure mode is similar to that of under-reinforced panels. Rahal [5] also considered the failure to be the

result of reinforcement yielding. The numerical analyses seem to be in accordance to the experiments, both in terms of post-cracking shear modulus and ultimate shear strength.

		$\tau_n / f_c^{'}$					
Specimen	ω_x/ω_y	Exp.	SMCS	Model	Exp/ SMCS	Exp/Mod.	SMCS /Mod.
A2	1.00	0.134	0.134	0.134	1.000	0.997	0.997
A3	1.00	0.192	0.192	0.192	1.000	0.999	0.999
VA1	1.00	0.068	0.056	0.056	1.214	1.214	1.000
VA2	1.00	0.104	0.100	0.100	1.040	1.037	0.997
VA3	1.00	0.167	0.173	0.173	0.965	0.965	1.000
PA1	2.01	0.127	0.122	0.129	1.041	0.981	0.942
PA2	2.02	0.145	0.142	0.150	1.020	0.964	0.945
B1	2.08	0.092	0.085	0.092	1.080	1.002	0.927
B2	1.40	0.146	0.151	0.154	0.967	0.951	0.984
B3	3.02	0.102	0.102	0.119	0.995	0.858	0.862
VB1	1.85	0.080	0.073	0.077	1.089	1.036	0.952
VB2	3.04	0.098	0.096	0.110	1.023	0.890	0.870
VB4	3.04	0.053	0.049	0.057	1.086	0.926	0.852
HB3	3.00	0.073	0.069	0.080	1.054	0.914	0.867
HB4	5.31	0.085	0.097	0.129	0.878	0.658	0.750

Table 2. Comparison of $\tau_n / f_c^{'}$ calculated by the numerical models versus experimental results and the SMCS.

		G_{cr}					
Specimen	ω_x/ω_y	Exp.	SMCS	Model	Exp/ SMCS	Exp/Mod.	SMCS/Mod.
A2	1.00	0.89	0.75	0.93	1.19	0.96	0.81
A3	1.00	1.25	1.08	1.25	1.16	1.00	0.86
VA1	1.00	0.69	0.72	0.95	0.96	0.73	0.76
VA2	1.00	1.37	1.33	1.63	1.03	0.84	0.81
VA3	1.00	2.14	2.21	2.41	0.97	0.89	0.92
PA1	2.01	0.69	0.82	1.05	0.84	0.66	0.78
PA2	2.02	0.75	0.83	1.03	0.91	0.73	0.80
B1	2.08	0.46	0.52	0.71	0.88	0.65	0.73
B2	1.40	0.95	0.90	1.10	1.06	0.86	0.82
B3	3.02	0.58	0.62	0.85	0.93	0.68	0.73
VB1	1.85	1.06	0.97	1.28	1.09	0.83	0.76
VB2	3.04	1.27	1.26	1.62	1.01	0.78	0.78
VB4	3.04	0.53	0.64	0.93	0.83	0.57	0.69
HB3	3.00	0.72	0.62	0.89	1.15	0.81	0.70
HB4	5.31	0.86	0.82	1.17	1.05	0.74	0.71

Table 3. Comparison of G_{cr} calculated by the numerical models versus experimental results and the SMCS.

PA series specimens by Vecchio et al. [10], shown in Figure 5, presented sliding shear failure of concrete immediately after yielding of the reinforcement in the weak direction, while localized yielding occurred in the strong one. Despite the localized failure of the weak direction, the failure mode of these two specimens can be categorized to that of under reinforced panels based on their response, as there is a distinct branch between yields in the $\tau - \gamma$ curve. Rahal [5] also considered the failure mode to be in this category. Vecchio et al. also

mention that the crack reorientation from the initial 45° was not noticeable. Moreover, the slope of the branch between yields in the numerical model with a shear retention factor of 0.25 is not in accordance to the one produced by the experiment. As the shear retention factor is responsible for crack reorientation and for the slope of the aforementioned branch, these facts lead to the conclusion that a shear retention factor of 0.25 overestimates the stiffness of the specimens. A shear retention factor of 0.15 leads to numerical results that fit better with the experimental ones.

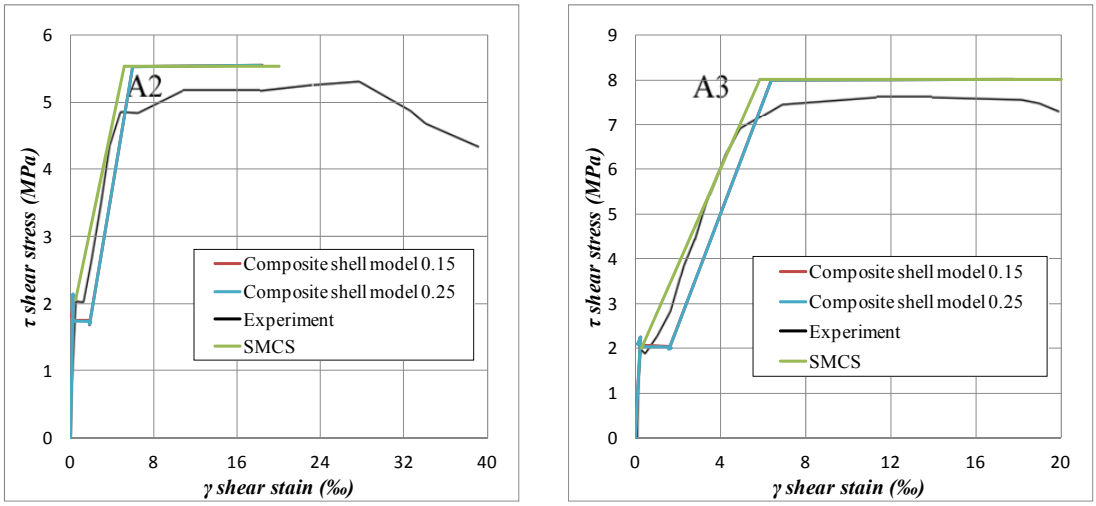

Figure 4. Experimental and numerical stress-strain curves for series A.

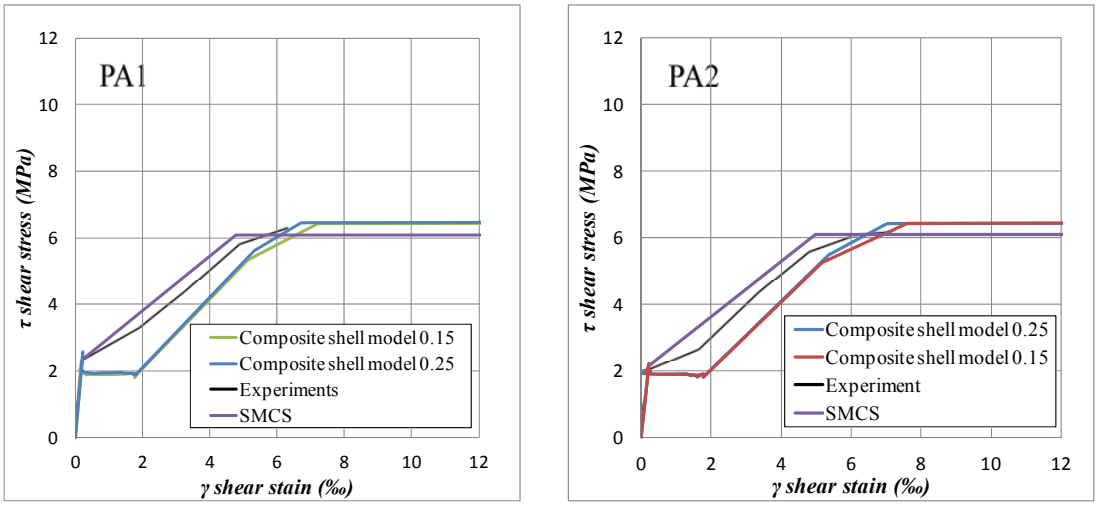

Figure 5. Experimental and model stress-strain curves for PA series.

In the comparison of the $\tau - \gamma$ curves yielded by specimens B1 to B3 tested by Pang and Hsu [9] to the numerically obtained curves (Figures 6 and 7), the first remark is the overestimation regarding the value of the shear retention factor in both cases ($\beta = 0.25$ and $\beta = 0.15$). Pang and Hsu mention that the heavily reinforced direction also yielded, which is also the case in the numerical models, thus the failure modes are in agreement. The yielding points of the two directions are overestimated by the numerical analyses and so is the ultimate shear strength. However, when the shear retention factor is equal to 0.15, the branch between yields produced by the numerical model is almost parallel to the corresponding branch of the experiment, although it starts at a higher shear stress. Thus, it seems that a value of β equal to 0.15 produces better results. The above mentioned differences in yielding points and ultimate shear strength become more obvious in the case of B3, in which the ratio of the reinforcement indices is higher. As aforementioned, these differences are caused by the violation of the cracking criterion. In the authors' opinion, the differences in cases B1 and B2 are within an acceptable range. In the case of B3, the differences, both in terms of ultimate shear strength and in terms of post cracking behavior, are not acceptable, but the SMCS also cannot capture the behavior of the specimen accurately.

Finally, in the case of the $\tau - \gamma$ curve of specimen HB3, shown in Figure 7, again the yielding of the reinforcements comes later in the numerical model, due to the concrete tensile stresses that arise as a result of the violation of the cracking criterion. A value $\beta > 0$ is necessary to take into consideration the contribution of concrete to the redistribution of the stresses and the complete neglect of shear retention would result in significant underestimation of the ultimate shear strength. However, the capacity was overestimated and the exact behavior of the model was not captured efficiently. The SMCS seems to reproduce the behavior of the specimen adequately.

A difference between the behavior of the numerical models and that of the majority of the specimens is located in the cracking region. All numerical models present a rapid transition between uncracked and cracked states, while in the experiments the transition is smoother and appears as a slightly less stiff branch between the elastic region and the region prior to first yield. This phenomenon is somehow inevitable, as the numerical model is based on the smeared crack theory and this leads to a rather even distribution of the stresses throughout the height of the tube and to a $\tau - \gamma$ diagram that concentrates all damage effects in a small region. However, in reality, due to the slight differences in the stress state and the material properties throughout the specimen, the onset of cracking occurs more progressively.

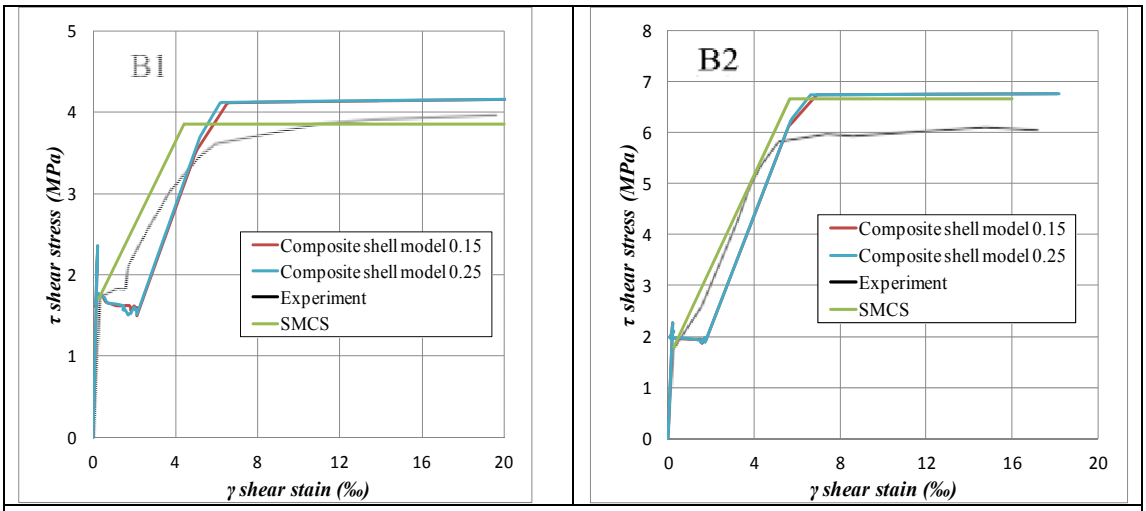

Figure 6. Experimental and model stress-strain curves for B1 and B2.

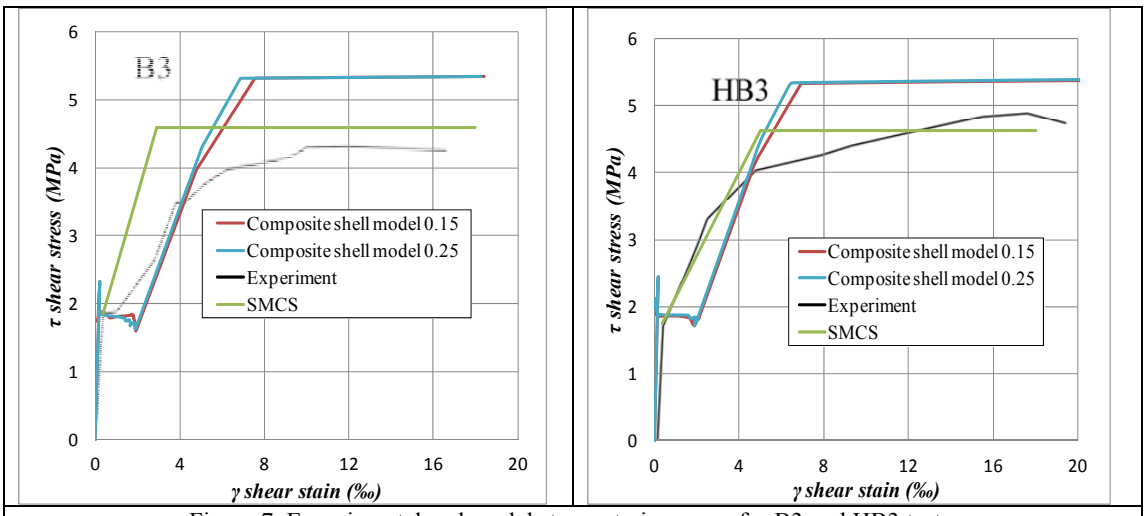

Figure 7. Experimental and model stress-strain curves for B3 and HB3 tests.

6 CONCLUSIONS

This study demonstrated a modeling technique for the analysis of ferrocement elements under in-plane shear which utilizes composite layered shell elements for the simultaneous simulation of the entire reinforced cross section. The simulation by composite shell elements offers a considerable flexibility in the carving of the actual

F.E. model, as there is no need for common nodes between elements representing the matrix and the ones used for the simulation the steel rods. The composite shell simulation technique cannot capture the slightly different behavior of elements with same reinforcement indices but different reinforcing patterns. However, as ferrocement elements are reinforced by meshes of closely spaced rods of small diameter, the resulting material is almost homogeneous and thus the mesh spacing does not play a significant role.

The comparison of the composite layered shell modeling method to existing experimental results and the Simplified Model for Combined Stress resultants (SMCS) demonstrated a very good agreement in the cases of reinforcement index ratios ω_x/ω_y up to 2. This range is similar to the one of the rotating-angle softened-truss model [11]. As far as shear retention is concerned, in the case of equal reinforcement indices the value assumed for β does not affect the results, as expected. However, as the ω_x/ω_y ratios become higher, shear retention causes the cracking criterion to be violated and the shear strength to be overestimated. This fact leads to the limitation of the presented simulation method to the aforementioned limit of $\omega_x/\omega_y \leq 2$. However, the reinforcement of ferrocement elements in most, if not all, cases comes in the form of square meshes and thus the ω_x/ω_y ratio is 1 or very close to unity. Hence, the range of application of the investigated simulation method can be considered to cover the majority of ferrocement structures and therefore can be applied with the confidence that the in-plane shear behavior is well approximated, given that the nonlinear modeling of the materials is included and an appropriate shear retention factor between 0.15 and 0.25 is taken into account.

REFERENCES

[1] Mitchell, D., Collins, MP. (1974), "Diagonal compression field theory-a rational model for structural concrete in pure torsion.", *ACI J Proc*, Vol. 71, pp. 396-408.

[2] Collins, MP. (1978), "Towards a rational theory for RC members in shear", *J Struct Div*, Vol. 104, pp. 649-666.

[3] Vecchio, FJ., Collins, MP. (1986), "The modified compression-field theory for reinforced concrete elements subjected to shear", *ACI J Proc*, Vol. 83, pp. 219-231.

[4] Bentz, EC., Vecchio, FJ., Collins, MP. (2006), "Simplified modified compression field theory for calculating shear strength of reinforced concrete elements", *ACI Struct J*, Vol. 103, pp. 614-624.

[5] Rahal, KN. (2008) "Simplified design and capacity calculations of shear strength in reinforced concrete membrane elements", *Eng Struct*, Vol. 30, pp. 2782-2791.

[6] Rahal, KN. (2010), "Post-cracking shear modulus of reinforced concrete membrane elements", *Eng Struct*, Vol 32, pp. 218-225.

[7] Bergan, PG. , Holand, I. (1979), "Nonlinear Finite Element Analysis Of Concrete Structures", *Comput Methods Appl Mech Eng*, Vol 17, pp. 443-467.

[8] MSC Software Corporation (2011), *MSC Marc, Volume A: Theory and user information*, MSC Software Corporation, USA.

[9] Pang, X., Hsu, TTC. (1995), "Behavior of reinforced concrete membranes in shear", *ACI Struct J*, Vol. 92, pp. 665-679.

[10] Vecchio, FJ., Collins, MP., Aspiotis, J. (1994), "High-strength concrete elements subjected to shear", *ACI Struct J*, Vol. 91, pp. 423-433.

[11] Hsu, TTC, Zhang, L. (1997), "Nonlinear analysis of membrane elements by fixed angle softened-truss model", *ACI Struct J*, Vol. 94, pp. 483-492.

[12] Hsu, TTC, Zhang, L. (1998), "Behavior and analysis of 100 MPa concrete membrane elements", *J Struct Eng*, Vol 124, pp. 24-34.

[13] Chaterjee, S., Adams, D., Oplinger, DW. (1993). *Test Methods for Composites: A Status Report. Volume 3: Shear Test Methods*, Blue Bell PA: MATERIALS SCIENCES CORP.

[14] Buyukozturk, O. (1977), "Nonlinear analysis of reinforced concrete structures", *Comput Struct*, Vol. 7, pp. 149-156.

[15] Rots, JG. (1988), *Computational modeling of concrete fracture*. PhD diss. Technische Hogeschool Delft.

[16] Hu, HT., Schnobrich, WC. (1190), "Nonlinear analysis of cracked reinforced concrete", *ACI Struct J*, Vol. 8, pp. 199-207.

[17] EN1992-1-2 (2004) *Eurocode 2: Design of concrete structures - Part 1-1: General rules and rules for buildings*, Brussels.